ELSEVIER

Journal of Power Sources 70 (1998) 28–33

JOURNAL OF POWER SOURCES

Characteristics of δ-$Ag_yV_2O_5$ as a lithium insertion host

Jin Kawakita *, Hiroko Sasaki, Mika Eguchi [1], Takashi Miura, Tomiya Kishi

Department of Applied Chemistry, Faculty of Science and Technology, Keio University, Hiyoshi 3-14-1, Kohoku-ku, Yokohama 223, Japan

Received 26 February 1997; accepted 11 March 1997

Abstract

δ-$Ag_yV_2O_5$ has been characterized as the active material for secondary lithium batteries by using electrochemical measurements and X-ray diffraction. Lithium insertion proceeds in three steps that include deposition of metallic silver and phase transformation to ϵ-$Li_xV_2O_5$. Metallic silver does not return to the original matrix during recharging. During the charge process, additional lithium is accommodated in the first and second steps. © 1998 Elsevier Science S.A.

Keywords: Silver; Vanadium; Secondary batteries; Lithium; Insertion; Extraction

1. Introduction

Vanadium oxides, such as V_2O_5 and V_6O_{13}, are promising cathode materials for lithium secondary batteries, and some of these compounds have been used commercially [1–4]. V_2O_5, however, has a drawback in that its crystal structure is easily destroyed during discharge and charge cycling. Many authors have reported the behaviour of more rigid host lattices with three-dimensional structures formed by the extraction of alkaline metal ions from the tunnel of β-$M_yV_2O_5$ (M = Li, Na and K) or by formation of complex oxides of V_2O_5 and other transition metal oxides such as molybdenum and silver oxides [5,6].

Silver vanadium oxide (SVO), $Ag_2V_4O_{11}$, which is a complex oxide of V_2O_5 and Ag_2O, has been used as a cathode material for primary lithium cells for implantable cardiac defibrillators [7–11]. The advantages of SVO are as follows: (i) less conductive material, such as carbon black, is required because metallic silver formed during the early stages of discharge increases the total conductivity of the cathode, and (ii) it is possible to discharge a large pulse current on a trace background current. Takeuchi and Thiebolt [7] reported the long-term discharge behaviour and West and Crespi [11] investigated changes in the crystal structure during discharge and charge.

An investigation has been made [12] of the lithium insertion behaviour of $Ag_{1+x}V_3O_8$ where Ag(I) occupies the octahedral sites between the layers. Ag(I) is reduced and deposited as metallic silver during the first step of discharge and, simultaneously, inserted Li(I) occupies the octahedral sites vacated by the Ag(I). Further Li^+ ions are inserted into the $Li_{1+x}V_3O_8$. In this case, formation of $Li_{1+x}V_3O_8$ is easily expected as it exists as a stable phase at ambient temperature. The authors also examined δ-$Ag_yV_2O_5$ which has a layer structure that is not isostructural with lithium bronzes, and investigated the effect of the insertion of Li(I) on changes in the crystal structure during discharge.

Garcia-Alvarado et al. [13,14] have reported the electrochemical performance of δ-$Ag_{0.68}V_2O_5$ when used as a cathode material for lithium secondary batteries. Takada et al. [15] have evaluated the suitability of δ-$Ag_yV_2O_5$ ($0.67 < y < 0.68$) as the active material for the electrode in a cell based on Ag^+ ions and using an inorganic solid electrolyte.

Garcia-Alvarado et al. [13,14] also reported the electrochemical lithium insertion behaviour of layered vanadium oxides prepared by extraction of Ag(I) from δ-$Ag_{0.68}V_2O_5$ by chemical oxidation. The behaviour of δ-$Ag_yV_2O_5$, however, was not well characterized compared with that of β-$Cu_{0.33}V_2O_5$ and ϵ-$Cu_{0.85}V_2O_5$. It is not clear, however, whether electrochemical oxidation enables Ag(I) to be extracted and what is the effect on the host lattice. Thus, the details of extraction of Ag(I) are also discussed in the work presented here.

* Corresponding author. Tel.: +81-45-563-11-41; fax: +81-45-563-04-46.

[1] Present address: National Research Institute for Metals, Sengen 1-2-1, Tsukuba 305, Japan.

PII S0378-7753(97)02615-3

2. Experimental

Andersson [16] has described a preparation method for δ-$Ag_yV_2O_5$ by hydrothermal synthesis. By contrast, Volkov et al. [17] obtained the compound by a solid-state reaction between Ag and V_2O_5 under an evacuated atmosphere. The δ-$Ag_yV_2O_5$ used in this paper was prepared by modifying the latter technique. A mixture of Ag_2O (Aldrich, > 99.99% purity), V_2O_5 (Junsei Chemical, > 99.0% purity) and V_2O_4 (Soekawa Chemicals, > 99.9% purity) in an appropriate ratio was pressed at 2×10^4 N cm^{-2} into a pellet and heated at 600 °C for 48 h in an evacuated quartz tube. The δ-$Ag_{0.75}V_2O_5$ was obtained after gradual cooling to room temperature at a rate of 0.42 °C min^{-1}. All the samples were characterized by powder X-ray diffraction (XRD) with a Rigaku apparatus (RINT 1300, Cu Kα radiation with nickel filter).

Electrochemical measurements were performed with a potentiostat/galvanostat (Toho Technical Research, 2092 and PS-08) in a cylindrical glass cell at 25 °C. All the cells were constructed in an argon-filled glove box. The counter and reference electrodes were metallic lithium rods (Aldrich, > 99.9% purity, 3.2 mm diameter). Both propylene carbonate (PC) and PC–dimethoxy ethane (DME) equivolume solutions containing 1 mol dm^{-3} $LiClO_4$ were used as the electrolytes (Mitsubishi Chemical, battery grade). The water content of the electrolytes was less than 20 ppm. The working electrode was prepared as follows. A powder of δ-$Ag_yV_2O_5$ was mixed with acetylene black (Denka black, Denkikagaku Kogyo) and poly(tetrafluoroethylene) (PTFE) in a weight ratio of 45:45:10, and the mixture was then pressed on a thin aluminum plate or porous nickel net at 2×10^4 N cm^{-2}. The latter served as a current collector and was connected to a copper lead by silver paste or gold paste. The surface on the opposite side of the collector was insulated with a silicone resin. After galvanostatic discharge and/or charge at a constant rate of 0.1 mA cm^{-2}, the open-circuit potential (OCP) was measured and its stationary value was obtained when the change was within 0.001 V h^{-1}. After the OCP measurement, ex situ XRD was run on a samples taken from the current collector and lead of the working electrode. Cyclic voltammetry was performed with a potentiostat and a function generator at a scan rate of 0.01 mV s^{-1}.

The amount of Ag^+ ions extracted into the electrolyte was determined by atomic absorption analysis (Hitachi, 180-55 AAS).

3. Results and discussion

3.1. Preparation of δ-$Ag_yV_2O_5$

Andersson [16] elucidated the structure of δ-$Ag_yV_2O_5$. The structure consists of layers which are composed of strongly distorted VO_6 octahedra that share edges and corners, as shown in Fig. 1. The layers have the composition V_2O_5 and are held together by means of Ag^+ ions, which are five-fold co-ordinated to oxygen atoms. Each layer consists of double zig–zag ribbons of octahedra with edges in common.

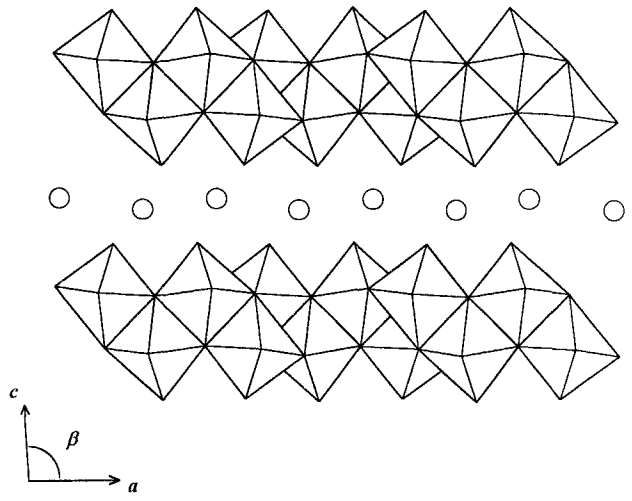

Fig. 1. Crystal structure of δ-$Ag_{1-y}V_2O_5$ [16]; open circles are silver atoms.

The XRD pattern of δ-$Ag_{0.75}V_2O_5$ obtained in this work is shown in Fig. 2. It agrees well with that of δ-$Ag_{1-x}V_2O_5$ ($x = 0.32$, monoclinic, $a = 11.742$ Å, $b = 3.677$ Å, $c = 8.738$ Å, $\beta = 90.48°$) indexed in the JCPDS card (No. 18-1194). The relative intensity of some peaks, however, is different from the data listed in the JCPDS card. In particular, a strong line appears at about $2\theta = 30°$ and is ascribed to diffraction of the (003) plane because of the preferred orientation.

3.2. Discharge and charge of δ-$Ag_yV_2O_5$

The discharge and the OCP curves of δ-$Ag_{0.75}V_2O_5$ are given in Fig. 3. Note that the value (x) on the abscissa in

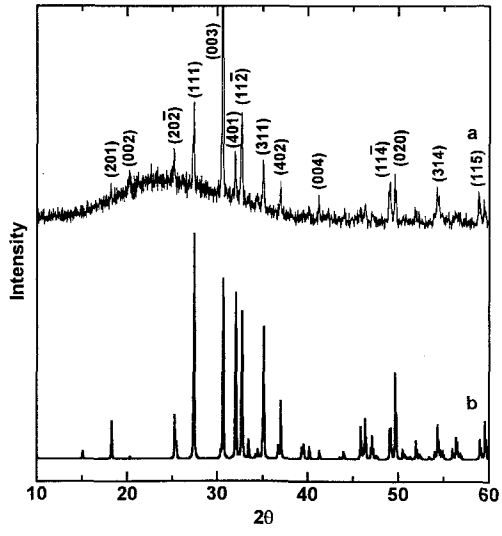

Fig. 2. (a) Observed ($y = 0.75$) and (b) calculated ($y = 0.68$) XRD patterns of δ-$Ag_{1-y}V_2O_5$.

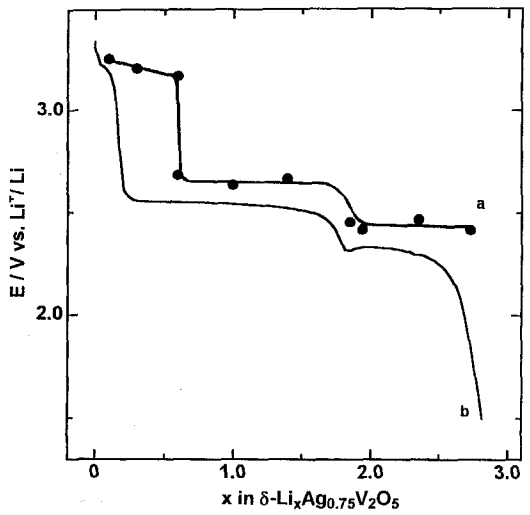

Fig. 3. (a) Open-circuit potential and (b) discharge curves of δ-$Ag_{1-y}V_2O_5$ at -0.1 mA cm^{-2}.

this profile indicates the amount of Li^+ ions inserted into δ-$Ag_{0.7}V_2O_5$ per a formula unit when all the electricity passed is consumed for lithium insertion reaction.

Three plateaus are observed at 3.2, 2.7 and 2.4 V in the OCP curve (see Fig. 3a) and on the corresponding discharge curve (Fig. 3b). Lithium insertion seems to proceed in the three steps. The discharge curve of δ-$Ag_yV_2O_5$ resembles that for ϵ-$Cu_yV_2O_5$ as reported by Garcia-Alvarado et al. [13,14] in terms of the shape. Presumably, this is because of the close relationship in the crystal structure of both vanadium oxides. Fig. 4 presents the XRD patterns of samples in which Li^+ ions are inserted electrochemically up to several x values. The peaks ascribed to the original material and metallic silver (marked by circles) appear in the range of the first plateau (see Fig. 3b), and metastable layered oxide with the composition of δ-$Li_xAg_{0.75-x}V_2O_5$ is formed by substituting Li(I) for part of the Ag(I). While the pattern assigned to metallic silver is observed clearly, that for the original phase decreases in the number of the diffraction lines at $x = 0.6$ where the second plateau begins. In contrast to $Ag_2V_4O_{11}$ (discussed later), not all of the Ag(I) species were reduced in the first plateau of the discharge curve of δ-$Ag_yV_2O_5$. At $x = 1.0$, new peaks (marked by arrows) appear beside the ones mentioned above. This indicates a formation of ϵ-LiV_2O_5. Thus, the original phase, metallic silver and ϵ-LiV_2O_5 coexist in the region of the second plateau. The peak near $2\theta = 30°$ disappears at both $x = 2.35$ and 2.85 in the region of the third plateau, but ϵ-LiV_2O_5 and metallic silver still remained. As yet, the peak near $2\theta = 17°$ has not been ascribed to any compound. From these results, lithium insertion into δ-$Ag_yV_2O_5$ in each plateau is summarized by the following equations:

(i) the first plateau ($0 \le x \le 0.6$)

$$\delta - Ag^+_{0.75}V^{4+}_{0.75}V^{5+}_{1.25}O_5 + xLi^+ + xe^- \rightarrow xAg^0 + \delta - Li^+_xAg^+_{0.75-x}V^{4+}_{0.75}V^{5+}_{1.25}O_5, \quad (1)$$

(ii) in the second plateau ($0 \le x' \le 0.15$, $0 \le x'' \le 1.0$)

$$\delta - Li^+_{0.6}Ag^+_{0.15}V^{4+}_{0.75}V^{5+}_{1.25}O_5 + (x' + x'')Li^+ + (x' + x'')e^- \rightarrow x'Ag^0 + (1 - x')\delta - Li^+_{0.6}Ag^+_{0.15}V^{4+}_{0.75}V^{5+}_{1.25}O_5 + x''\epsilon - Li^+_{0.6+x'+x''}V^{4+}_{0.75+x''}V^{5+}_{1.25-x''}O_5, \quad (2)$$

and (iii) in the third plateau ($0 \le x''' \le 0.25$, $0 \le x'''' \le 0.75$)

$$\epsilon - Li^+_{1.75}V^{4+}_{1.75}V^{5+}_{0.25}O_5 + (x''' + x'''')Li^+ + (x''' + x'''')e^- \rightarrow \epsilon - Li^+_{1.75+x'''+x''''}V^{3+}_{x''''}V^{4+}_{1.75+x'''-x''''}V^{5+}_{0.25-x'''}O_5. \quad (3)$$

The galvanostatic discharge and charge curves of δ-$Ag_{0.75}V_2O_5$ are given in Fig. 5. The charge curve shows steps of the type observed for ϵ-$Cu_{0.85}V_2O_5$ [13,14]. When the discharge and charge cycle is performed over a shallow depth-of-discharge (DOD) to a cut-off voltage of 2.4 V, the original material remains and the diffraction line of the (003) plane is shifted to a high angle, as shown in Fig. 6b. Extraction of Li^+ between the layers of $Li_xAg_{0.75-x}V_2O_5$ causes a decrease in interlayer distance. For cycling to a deep DOD (cut-off voltage of 1.5 V), diffraction lines of a new phase in addition to metallic silver appeared in the XRD pattern (see Fig. 6c). This behaviour is different to that for $Ag_2V_4O_{11}$ as reported by West and Crespi [11]. In the latter study, deposited Ag(0) was reoxidized and returned to the original material. The peaks of an unidentified new phase (marked by arrows) do not agree with

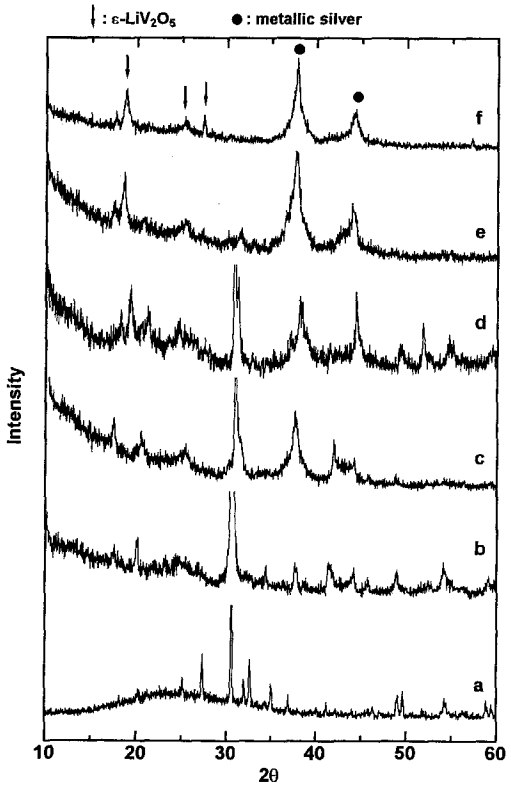

Fig. 4. XRD patterns of lithiated samples $Li_xAg_{0.75}V_2O_5$: (a) $x = 0$; (b) $x = 0.1$; (c) $x = 0.3$; (d) $x = 1.0$; (e) $x = 2.35$; and (f) $x = 2.82$.

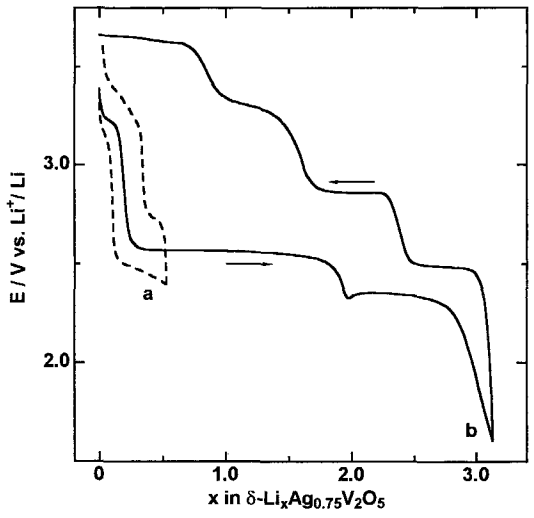

Fig. 5. First discharge and charge cycle curves of δ-$Ag_{0.75}V_2O_5$ at ± 0.1 mA cm^{-2} with cut-off voltage of (a) 2.4 V and (b) 1.5 V.

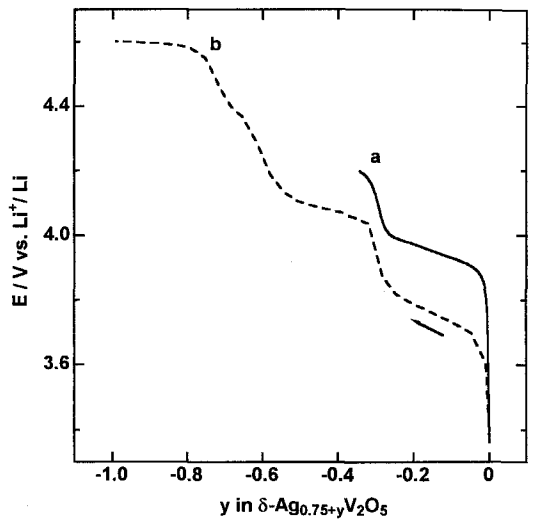

Fig. 7. Charging curves of δ-$Ag_{0.75}V_2O_5$ at ± 0.1 mA cm^{-2} up to (a) 4.2 V in 1 M $LiClO_4$/PC and (b) 4.6 V in 1 M $LiClO_4$/PC-DME.

those of ϵ-LiV_2O_5 formed as the result of discharge. Broadening of the peaks of the new phase in the XRD pattern indicate that extraction of silver and insertion/extraction of lithium causes destruction of the host lattice.

3.3. Charge and discharge of δ-$Ag_yV_2O_5$

On anodic galvanostatic polarization, Ag(I) is able to be extracted, as shown in Fig. 7. The first plateau potentials are different for PC and PC/DME electrolytes. It is found that extraction of silver proceeds in two steps up to 4.6 V where decomposition of electrolyte occurs. The amount of extracted silver (determined by atomic absorption analysis) is smaller than the value calculated from the quantity of charge passed. Presumably, oxidation of Ag(I) to Ag(II) remaining in the host lattice takes place at the second plateau in the charge profile. XRD patterns of the silver-extracted sample are shown in Fig. 8. At the end of the first plateau, the existence of the host structure is observed in the pattern (Fig. 8c) and the original phase is maintained. The peaks near $2\theta = 18$, 25, 32 and 41° are ascribed to the diffraction lines of the (201), (202), (003) and (004) planes, respectively. These peaks are strengthened in their relative intensities as the extraction process continues. This phenomenon can be explained in terms of both the position and the number of silver atoms in the host lattice. As seen in Fig. 1, the double layer of this oxide consists of stacking in the c direction on the a–b plane and silver atoms exist between the layers. Accordingly, extraction of

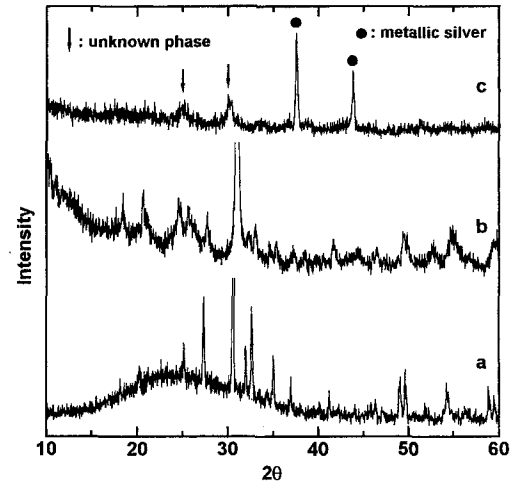

Fig. 6. XRD patterns of δ-$Ag_{0.75}V_2O_5$ (a) as starting material, and after first discharge and charge cycle with cut-off potential of (b) 2.4 V and (c) 1.5 V.

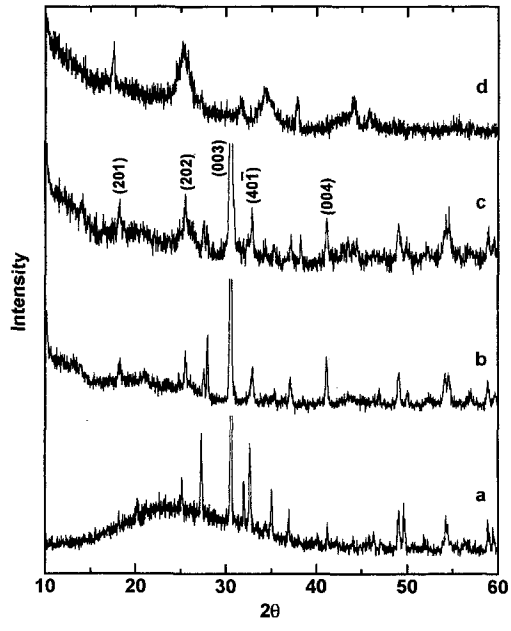

Fig. 8. XRD patterns of δ-$Ag_{0.75}V_2O_5$ (a) as starting material, and charged up to (b) 4.0 V, (c) 4.2 V in 1 M $LiClO_4$/PC, and (d) 4.6 V in 1 M $LiClO_4$/PC-DME.

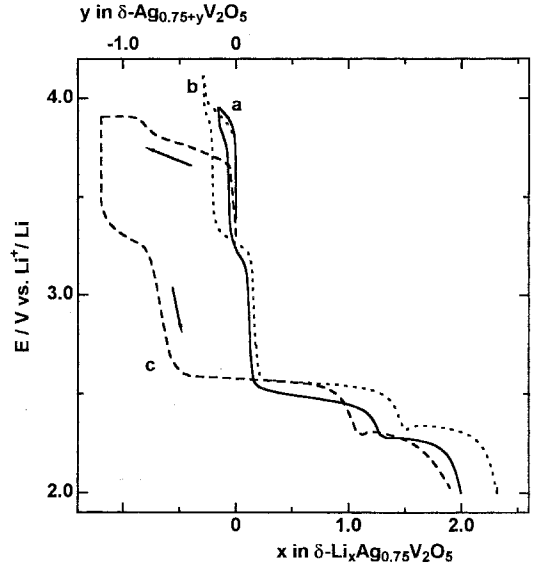

Fig. 9. First charge and discharge cycle curves of δ-$Ag_{0.75}V_2O_5$ at ± 0.1 mA cm^{-2} with cut-off voltage of (a) 4.0 V and (b) 4.2 V in 1 M $LiClO_4$/PC, and (c) 3.9 V in 1 M $LiClO_4$/PC-DME.

silver increases the intensity of the diffraction lines of the $(h0l)$ and $(00l)$ planes. When charged to a high potential of 4.6 V, all the peaks are broadened and the diffraction lines of the $(00l)$ plane disappear, as seen in Fig. 8(d). This probably indicates partial destruction of the crystal structure by too much extraction of Ag atoms from connecting adjacent layers. Thus, it is found that δ-$Ag_yV_2O_5$ maintains its crystal structure, even if charged up to a high potential of 4.2 V.

The effects of the extraction of Ag(I) by anodic polarization on the discharge behaviour are shown in Fig. 9. The plots in Fig. 10 show the relationship between the amount of extracted silver and that of lithium inserted at the first (near 3.2 V) and the second (near 2.5 V) plateaus in Fig. 9. It is found that the region of the first plateau in the discharge curves is extended in proportion to the increase in amount of extracted silver during charging. Otherwise, when the sum of the guest species situated between the layers of the original material is greater than about 0.9, a second phase is formed because δ-$M_yV_2O_5$-type oxides that include only lithium do not exist as a stable phase (this vanadium oxide is different from $Ag_{1+x}V_3O_8$ in this respect). The amount of inserted lithium in the region of the second plateau also increases linearly with the amount of extracted silver. This fact is supported by the deduction that lithium is easier to be inserted into the stable ϵ-LiV_2O_5 phase than into unstable δ-$M_yV_2O_5$ that contains Ag(I) and Li(I). The XRD patterns of the sample after charge/discharge cycling to various cut-off voltages are shown in Fig. 11. Both ϵ-LiV_2O_5 and metallic silver appear mainly at the end of the cycle irregardless of the cut-off potentials of charging. Moreover, some unknown peaks are also observed in the patterns. It is difficult to identify the new phase derived from these peaks because of their broadening and weak intensities.

The cyclic voltammogram of δ-$M_yV_2O_5$ is given in Fig. 12. On the first cycle, three cathodic peaks appear at about 3.2, 2.4 and 2.1 V. These peaks correspond to the plateau region in the discharge curve shown in Fig. 3(b). The three anodic peaks observed near 2.5, 3.0 and 3.4 V on the first cycle do not shift on third cycle. Thus, lithium is reversibly inserted to and extracted from ϵ-LiV_2O_5 formed after finishing the potential scan in the cathodic direction

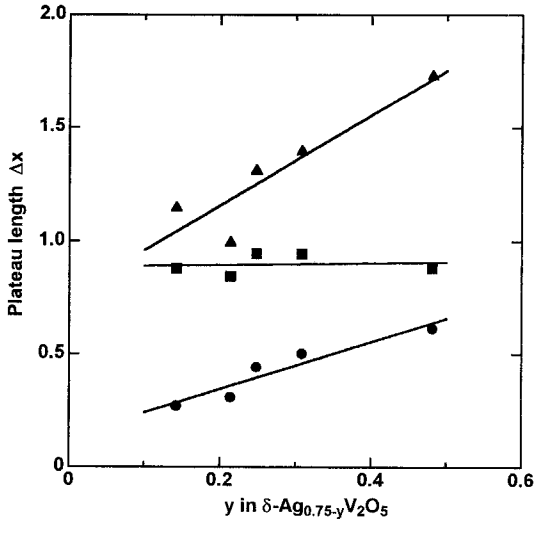

Fig. 10. Relation between amount of extracted silver and plateau length during discharge. (●) Δx_1 at the first plateau; (■) $0.75 - y + \Delta x_1$, (▲) Δx_2 at the second plateau.

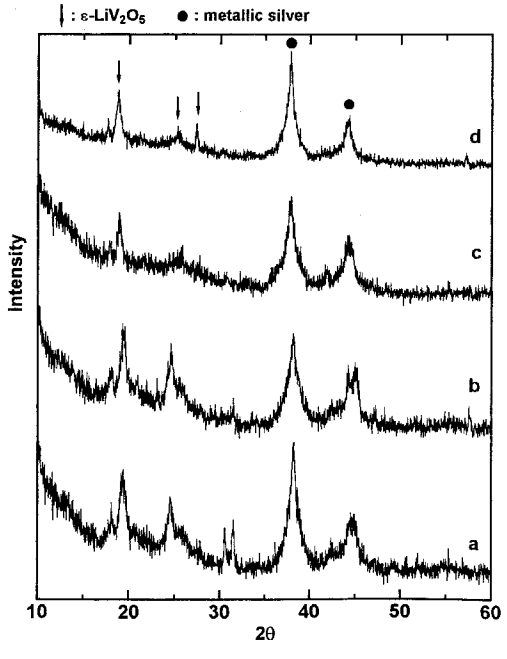

Fig. 11. XRD patterns of δ-$Ag_{0.75}V_2O_5$ after the first charge and discharge cycle curves with cut-off voltage of (a) 4.0 V, (b) 4.2 V in 1 M $LiClO_4$/PC, (c) 3.9 V in 1 M $LiClO_4$/PC-DME, and (d) only discharged in 1 M $LiClO_4$/PC.

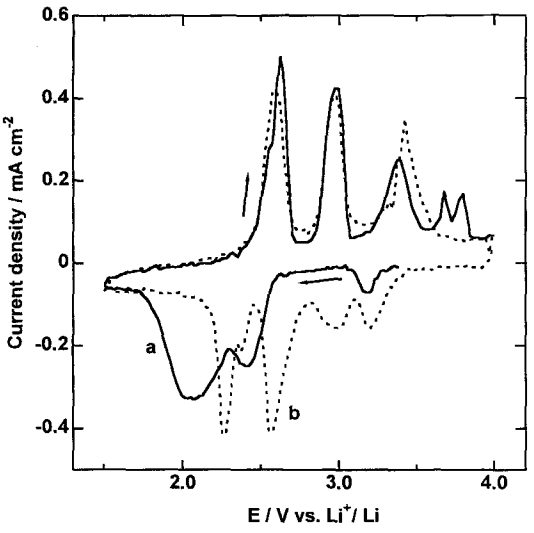

Fig. 12. Cyclic voltammograms of δ-$Ag_{0.75}V_2O_5$ at 0.01 mV s^{-1} at (a) first cycle, and (b) third cycle.

on the first cycle. It is concluded that the additional two anodic peaks observed at potentials above 3.6 V on the first cycle are due to oxidation from Ag(0) to Ag(I), and further to Ag(II).

4. Conclusions

During discharge, about three moles of Li^+ ions are inserted into δ-$Ag_yV_2O_5$ in three regions that are distinguished by plateau potentials. In the first region, Ag(I) between the layers are reduced to Ag(0) and deposited as metallic silver, and inserted Li^+ ions occupy the available sites between the layers. In the second region, the δ-$Ag_yV_2O_5$ phase changes to ϵ-$Li_xV_2O_5$ with lithium insertion in addition to reduction of Ag(I). In the third region, additional Li^+ ions are accommodated in the ϵ-$Li_xV_2O_5$.

Ag(0) does not return to the vanadate during recharging once metallic silver formed. Although cyclic voltammetry shows good reversibility of the sample after the second cycle, it is difficult to determine the details of its structural change due to broadening of diffraction lines in the XRD pattern with cycling.

During the oxidation process, Ag(I) can be extracted from the interlayers of δ-$Ag_yV_2O_5$. Furthermore, additional Li^+ ions are inserted in the first and second regions in proportion to the amounts of extracted Ag(I). This confirms that Ag(I) is reduced not only in the first but also in the second region.

References

[1] D.W. Murphy, P.A. Christian, F.J. DiSalvo, J.N. Carides, J. Electrochem. Soc. 126 (1979) 497.
[2] K.M. Abraham, J.L. Goldman, M.D. Dempsy, J. Electrochem. Soc. 128 (1981) 2493.
[3] N. Kumagai, K. Tanno, T. Nakajima, N. Watanabe, Electrochim. Acta 28 (1983) 17.
[4] Y. Muranushi, T. Miura, T. Kishi, T. Nagai, Denki Kagaku 54 (691) (1986) 123.
[5] B. Zachau-Christiansen, K. West, T. Jacobsen, Solid State Ionics 9/10 (1983) 399.
[6] K. West, B. Zachau-Christiansen, S. Skaarup, T. Jacobsen, Solid State Ionics 53/56 (1983) 356.
[7] E.S. Takeuchi, W.C. Thiebolt III, J. Electrochem. Soc. 135 (1988) 2691.
[8] E.S. Takeuchi, W.C. Thiebolt III, J. Electrochem. Soc. 138 (1991) L44.
[9] R.A. Leising, E.S. Takeuchi, Chem. Mater. 5 (1993) 738.
[10] A.M. Crespi, P.M. Skarstad, H.W. Zandbergen, J. Power Sources 54 (1995) 68.
[11] K. West, A.M. Crespi, J. Power Sources 54 (1995) 334.
[12] J. Kawakita, Y. Katayama, T. Miura, T. Kishi, Solid State Ionics, in press (1997).
[13] F. Garcia-Alvarado, J.M. Tarascon, B. Wilkens, J. Electrochem. Soc. 139 (1992) 3206.
[14] F. Garcia-Alvarado, J.M. Tarascon, Solid State Ionics 63/65 (1993) 401.
[15] K. Takada, T. Kanbara, Y. Yamaura, S. Kondo, Denki Kagaku 58 (1990) 324.
[16] S. Andersson, Acta Chem. Scand. 19 (1965) 1371.
[17] V.L. Volkov, A.A. Fotiev, N.G. Fedotovskikh, E.I. Andreikov, Russ. J. Phys. Chem. 48 (1974) 887.